IOP PUBLISHING JOURNAL OF PHYSICS D: APPLIED PHYSICS

J. Phys. D: Appl. Phys. **46** (2013) 145104 (7pp) doi:10.1088/0022-3727/46/14/145104

Quantitative analysis of the contribution of nanocone gratings to the efficiency of crystalline Si thin-film solar cells

R Y Zhang, Z Zhang, B Shao, J R Dong and H Yang

Key Lab of Nanodevices and Applications, Chinese Academy of Sciences, Division of nano-devices and related materials, Suzhou Institute of Nano-tech and Nano-bionics, Chinese Academy of Sciences, Suzhou 215123, People's Republic of China

E-mail: ryzhang2008@sinano.ac.cn

Received 25 October 2012, in final form 27 January 2013
Published 11 March 2013
Online at stacks.iop.org/JPhysD/46/145104

Abstract

Quantitative analysis of the contribution from different physics mechanisms induced by nanocone gratings (NCG) to the efficiency of crystalline Si thin-film solar cells is systematically demonstrated through the performance comparison of such a nanotextured Si solar cell, an equivalent reflection planar Si solar cell, an equivalent volume planar Si solar cell and an actually planar Si solar cell, when their back-interface is a perfect-matched layer or air and their thickness is 1 μm or 10 μm. The results indicate that the contribution of each physics mechanism to the ultimate efficiency and their total contribution are significantly influenced by the thickness of their active layer. When the height of the NCG structure is comparable to the thickness of the active layer, the contribution from each physics mechanism to the efficiency must be considered. In that respect, the contribution from the guided-mode resonance effect is the largest, and even surpasses the contribution of the active layer itself. When the active layer is significantly thicker than the height of the NCG structure, the contribution from antireflection induced by such a nanostructure rises up to the most, and the volume reduction effect can be ignored. In addition, the cavity-resonance effect exhibits a weak contribution and seems to be insensitive to the active layer thickness and interface reflection. Such an investigation provides a methodology to optimize nanostructure-textured thin-film solar cells. Furthermore, the comparison of efficiency between a 1 μm thick NCG-textured solar cell and a 10 μm thick planar solar cell indicates that higher efficiency can be achieved in a thinner Si solar cell by the use of the optimized NCG structure, which just fulfils the expectation of third generation of Si solar cells.

(Some figures may appear in colour only in the online journal)

1. Introduction

The material cost of the first generation solar cells and the efficiency limitation of the second generation solar cells have initiated the research on Si-based third generation photovoltaics, which aims at significantly increasing the conversion efficiencies while still using thin-film processes For Si-based thin-film solar cells with an active layer of several micrometres thick, effectively reducing the optical absorption loss, which mainly consists of reflection loss due to their high refractive index and high transmission loss over a longer wavelength domain due to their indirect bandgap, is one of the main strategies to enhance their conversion efficiencies. According to the requirements of specific thickness and high efficiency, different photonic management (PM) methods based on dielectric nanophotonic structures, such as photonic crystal structures [1–3], nanowires (nanorods) [4–8], nanopores [9] and nanocone structures [10–15], have been proposed and investigated in Si-based solar cells [1–15]. The corresponding structures have been optimized and their underlying physics have been qualitatively explored [1–3, 8–12, 15]. Overall, four physical mechanisms make contribution to the variation of their absorption and efficiency. Generally speaking, broadband antireflection, guided-mode resonance

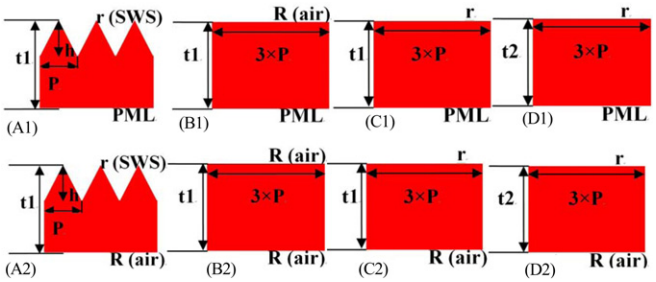

Figure 1. Schematic simulation models of the NCG-textured Si solar cell and its counterparts. The back-surface is a PML for (A1), (B1), (C1) and (D1); the back-interface is air for (A2), (B2), (C2) and (D2).

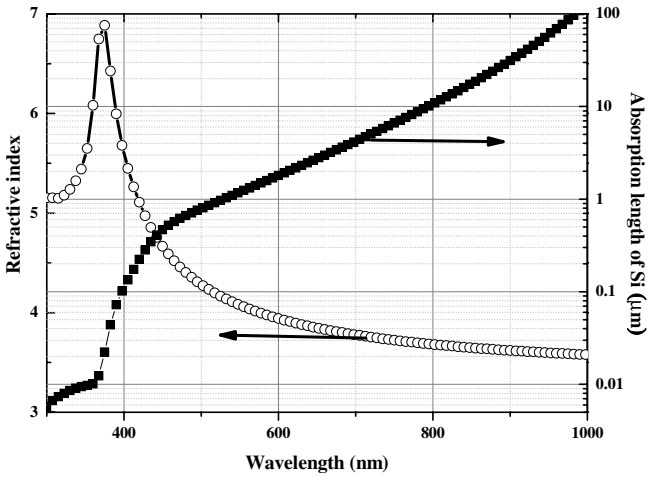

Figure 2. Refractive index and absorption length of the Si material at different wavelengths.

and cavity oscillation enhance the absorption and conversion efficiency, but volume reduction degrades their performance. However, to the best of our knowledge, there has been no quantitative analysis of each physical mechanism contribution to the efficiency enhancement in any nanostructured solar cell, which is important for solar cells to enhance their conversion efficiency through PM methods.

Moreover, compared with other nanophotonic structures, nanocone structures are very attractive for Si thin-film solar cells due to their broadband antireflection and light trapping in the longer wavelength domain [10–12, 15]. We systematically investigated the influence of the period and height of nanocone gratings (NCG) on the performance of 1 μm thick NCG-textured Si solar cells [15]. There the physics mechanism of absorption enhancement and ultimate efficiency enhancement was discussed and an optimized NCG structure with period of 560 nm and height of 500 nm was achieved.

In this paper, the above-mentioned optimized NCG structure is employed in 1 and 10 μm thick crystalline Si solar cells. The contribution from each physical mechanism to the improvement of their absorption and ultimate efficiency is quantitatively explored through the comparison of their performance in different simulation models operated with different back-interfaces. The results clearly show that the guided-mode resonance excited by high-order diffraction of the NCG dominates the absorption and efficiency enhancement in such 1 μm thick Si solar cells, and accounts for 54.17% of the total ultimate efficiency, but the antireflection contribution is the most in 10 μm thick Si solar cells, accounting for 28.68% of the total ultimate efficiency. Such a quantitative analysis should benefit the optimization of crystalline Si thin-film solar cells through the PM method. Moreover, such a strategy can be widely employed to the advanced design of other thin-film solar cells.

2. Simulation

To study the contribution from each physics mechanism to the absorption and efficiency, eight different simulation models, as shown in figure 1, are adopted in this paper. Here, (A1) and (A2) in figure 1 show the Si solar cells, which consist of a top close-packed NCG structure and an underlying planar film. For this, an NCG structure with a period (P) of 560 nm and a height (h) of 500 nm is selected, which is the optimized structure for 1 μm thick Si solar cells according to our prior analysis [15]. As a reference, 1 μm thick planar Si solar cells with front-surface reflectivity of R are shown in (B1) and (B2) of figure 1. The models that have a dummy front interface with reflectivity of r (λ), the same as that of the NCG structure, are shown in (C1) and (C2) of figures 1, and are called the effective reflection planar Si solar cells. As the variation of absorption and efficiency is also related to the volume variation induced by the NCG pattern, planar Si solar cells with the same interface as that of (C1) and (C2), but with the same volume as that of (A1) and (A2), are shown in (D1) and (D2) of figure 1, and are called the effective volume planar Si solar cells.

To further quantitatively investigate the influence of cavity-resonance contribution on the efficiency variation, a perfect-matched layer (PML) is selected as the back-interface for (A1), (B1), (C1) and (D1) of figure 1, while air is selected as the back-interface for (A2), (B2), (C2) and (D2) of figure 1. Moreover, for the 1 μm thick Si solar cell, $t1 = 1\,\mu$m and $t2 = 0.6309\,\mu$m, while for the 10 μm thick Si solar cell, $t1 = 10\,\mu$m and $t2 = 9.6309\,\mu$m.

To match the silicon absorption spectrum, a wavelength range from 300 to 1000 nm was selected. Si optical constants measured by an MD2000D spectroscopic ellipsometer were used in such simulations. Moreover, the Si absorption length is calculated according to the above Si absorption coefficient. The refractive index and absorption length of the Si material at different wavelengths are shown in figure 2.

As before [15], only the normalized incidence is considered in this paper. The absorption of NCG-based Si solar cells is numerically simulated through a rigorous coupled-wave analysis (RCWA). The absorption of planar Si solar cells is simulated by the transmission matrix method (TMM). Based on the above achieved absorption spectrum, and assuming that each photon absorbed by the Si material can generate an electron–hole pair, the ultimate efficiency, η, is calculated as follows [16]:

$$\eta = \frac{\int_0^{\lambda_g} f(\lambda)A(\lambda)(\lambda/\lambda_g)\,\mathrm{d}\lambda}{\int_0^{\infty} f(\lambda)\,\mathrm{d}\lambda} \qquad (1)$$

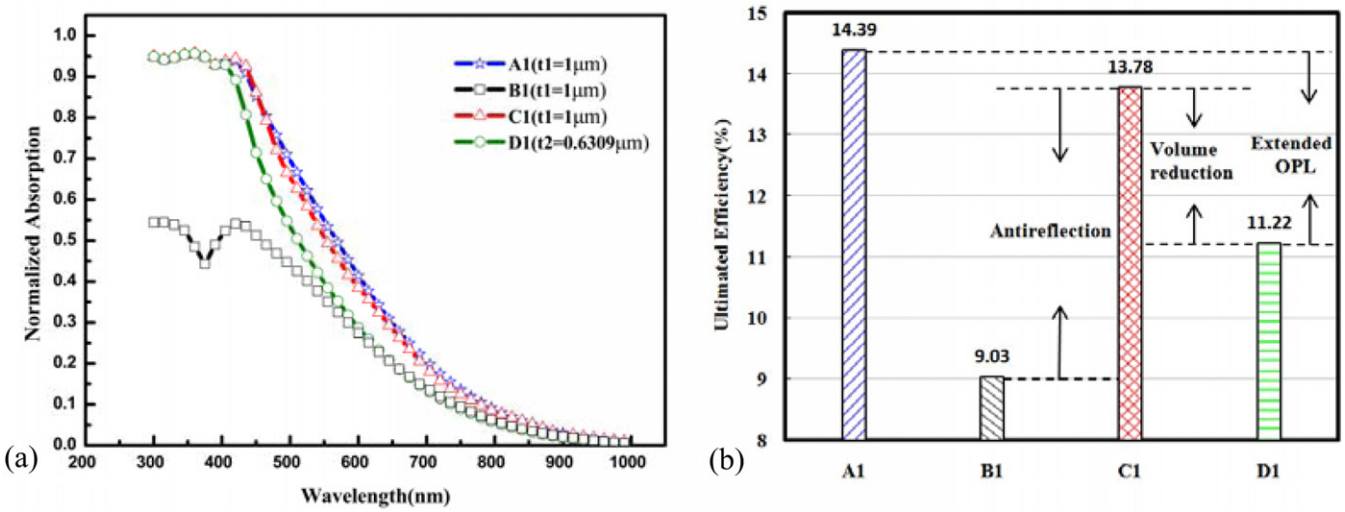

Figure 3. (*a*) Normalized absorption spectra. (*b*) Ultimate conversion efficiency and physics mechanisms for models A1, B1, C1 and D1 ($t1 = 1\,\mu$m, $t2 = 0.6309\,\mu$m).

where λ_g is the wavelength corresponding to the bandgap, $f(\lambda)$ is the incident photon flux (number of photons incident per unit area per second per wavelength) of AM1.5D, $A(\lambda)$ is the normalized absorption intensity of the above-mentioned Si solar cells, which is simulated by RCWA for models A1 and A2, and simulated by the TMM for the other models.

3. Results and discussion

3.1. 1 μm thick crystalline Si solar cells

3.1.1. PML back-interface. The normalized absorption of models A1, B1, C1 and D1 in figure 1 is shown in figure 3. The back-interface is a PML, which means there is single-pass absorption for any incident light in such a structure. Significantly, the same absorption is observed in the models with the same front-interface reflectivity r, and each value is considerably higher than that of the pure planar Si solar cell when the incident wavelength (λ_{in}) is less than 400 nm, which indicates the front-interface reflection is the only absorption loss in this wavelength domain. Even though the absorption of the pure planar Si solar cell is always lower than that of the other models, the difference becomes gradually smaller with increasing λ_{in}, which means the role of front-interface reflection in the total absorption loss becomes gradually weaker. When $\lambda_{in} > 400$ nm, even though models C1 and D1 have the same front-interface reflectivity, the absorption of model C1 is higher than that of model D1, but the difference becomes small with an increase in λ_{in}, which means volume reduction is one of the absorption loss mechanisms and its influence on absorption becomes weaker and weaker. Furthermore, even though models A1 and D1 have the same volume and interface reflectivity, the absorption of model A1 is higher than that of model D1 when $\lambda_{in} > 400$ nm, which reveals that such an absorption enhancement is due to the extended optical path length (OPL) induced by high-order diffraction in the NCG structure. In addition, the absorption of model C1 is higher than that of model A1 over most of the wavelength range, which means the absorption degradation induced by volume reduction is stronger than the enhancement induced by the extended OPL.

The overall ultimate conversion efficiency of different models calculated as equation (1) at AM1.5 is shown in figure 3(*b*). Moreover, the efficiency variation induced by each physics mechanism is also clearly demonstrated here. As expected, the efficiency of the NCG-textured 1 μm thick Si solar cell (model A1) is significantly higher than that of the 1 μm thick planar Si solar cell (model B1), even though there is only single-pass absorption. The contribution of antireflection to the efficiency enhancement is 4.75%, derived from the value difference of models B1 and C1. The efficiency degradation due to volume reduction for the NCG-textured Si solar cells is 2.56%, derived from the value difference of models C1 and D1. In addition, the contribution of extended OPL induced by the NCG structure to the efficiency enhancement is 3.17%, derived from the value difference of models A1 and D1. Overall, the above quantitative analysis indicates that the ultimate efficiency of an NCG-based solar cell is determined by the antireflection, volume reduction and extended OPL, except for the Si material itself.

3.1.2. Air back-interface. The normalized absorption of models A2, B2, C2 and D2 in figure 1 is shown in figure 4(*a*). As the back-interface of these models is air, models A2 and B2 are the real operation states of the NCG-textured and planar Si solar cells. As expected, the highest absorption over the whole spectra and the highest ultimate conversion efficiency are exhibited by the NCG-textured Si solar cells. When λ_{in} is less than about 450 nm, the models with the same front-interface reflectivity have the same absorption, considerably higher than that of model B2, which indicates that the front-interface reflection is the only absorption loss in this wavelength domain due to their absorption length of less than 2 μm. After that, the absorption oscillation spectra are observed in these models as their absorption length is longer than its effective active layer thickness. The absorption oscillation spectra of models B2, C2 and D2 are periodically induced by the cavity-resonance effect.

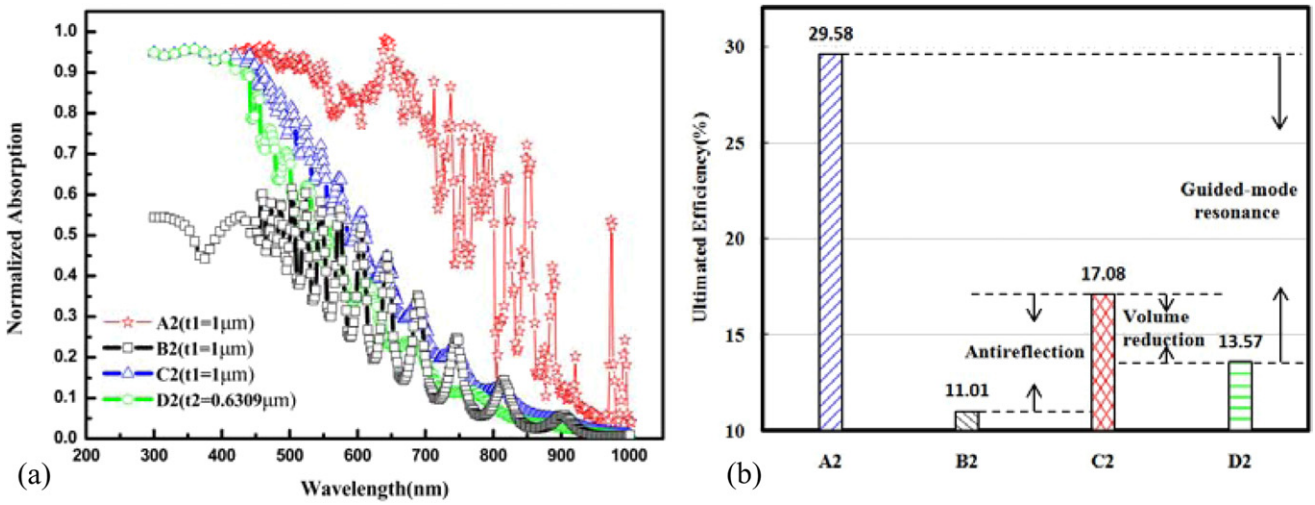

Figure 4. (*a*) Normalized absorption spectra. (*b*) Ultimate conversion efficiency and physics mechanisms for models A2, B2, C2 and D2 ($t1 = 1\,\mu$m, $t2 = 0.6309\,\mu$m).

Moreover, the same period oscillation spectra are observed in models B2 and C2 due to the same active layer thickness. However, the absorption intensity of model C2 is higher than that of model B2 due to its lower front-interface reflectivity. In addition, the absorption intensity of model C2 is higher than that of model D2 due to their volume difference. Compared with the spectra of other models, the absorption of model A2 is significantly higher and exhibits aperiodic oscillation due to the participation of guided-mode resonance induced by the higher order diffraction. For models A2 and D2, even though they have the same volume and interface reflectivity, the absorption intensity of model A2 is considerably higher than that of model D2, which indicates that guided-mode resonance induced by the higher order diffraction makes the greater contribution to the absorption enhancement.

Meanwhile, the overall ultimate efficiency of models A2, B2, C2 and D2 is shown in figure 4(*b*). As expected, the highest efficiency of nearly 30% is achieved in the 1 μm thick NCG-textured Si solar cell. This value is much higher than that of the other models, which indicates that the guided-mode resonance plays an important role in the ultimate efficiency enhancement. In order to further probe the efficiency enhancement, physics mechanisms that induce the efficiency variation are also clearly demonstrated here. As shown in figure 4(*b*), the efficiency of a 1 μm thick NCG-textured Si solar cell is 18.57% higher than that of a planar Si solar cell, derived from the value difference of models A2 and B2. The contribution of antireflection to the efficiency enhancement is 6.07%, derived from the value difference of models B2 and C2. The efficiency degradation induced by volume reduction is 3.51%, derived from the value difference of models C2 and D2. In addition, the contribution of guided-mode resonance induced by the NCG structure to the efficiency enhancement is 16.01%, derived from the value difference of models A2 and D2. Moreover, a comparison of the models with different back-interfaces (PML and air) is shown in table 1. For Si solar cells with a planar structure, the efficiency enhancement induced by the cavity-resonance effect is about 1.98–2.69%. For NCG-textured Si solar cells, the efficiency enhancement increases to 15.80%. In that case, the contributions from the cavity-resonance effect and the guided-mode effect are 2.35% and 13.45%, respectively. The guided-mode effect induced by high-order diffraction significantly improves the absorption and efficiency of such 1 μm thick NCG-textured crystalline Si solar cells.

Table 1. Comparison of the efficiency of simulation models with different back-interfaces (PML and air).

η (%)	Model A	Model B	Model C	Model D
PML	13.78	9.03	14.39	11.22
Air	29.58	11.01	17.08	13.57
$\Delta\eta$ (%)	15.80	1.98	2.69	2.35

3.2. 10 μm thick crystalline Si solar cells

In order to investigate the influence of active layer thickness on the physics mechanism contribution to the enhancement of absorption and efficiency, a similar simulation was conducted on 10 μm thick crystalline Si solar cells. The simulation models are shown in figure 1, and here $t1 = 10\,\mu$m and $t2 = 10–0.3691 = 9.6309\,\mu$m; other parameters are the same as before.

3.2.1. PML back-interface. The normalized absorption and ultimate efficiency of models A1, B1, C1 and D1 are shown in figure 5(*a*). As all the above models have the same back-interface of PML, the incident lights have to experience single-pass absorption. Significantly, the absorption intensity of the planar Si (model B1) is lower than that of the other models over the whole span due to its higher front-interface reflection. Nearly overlapped absorption curves are observed for models C1 and D1 when $\lambda_{in} < 700$ nm, which indicate that front-interface reflection completely dominates the absorption in this wavelength domain. Moreover, its normalized absorption intensity is much higher than its counterpart in figure 3(*a*) over the whole span due to its thicker active layer. When $\lambda_{in} \geqslant 700$ nm, model A1 exhibits the highest absorption

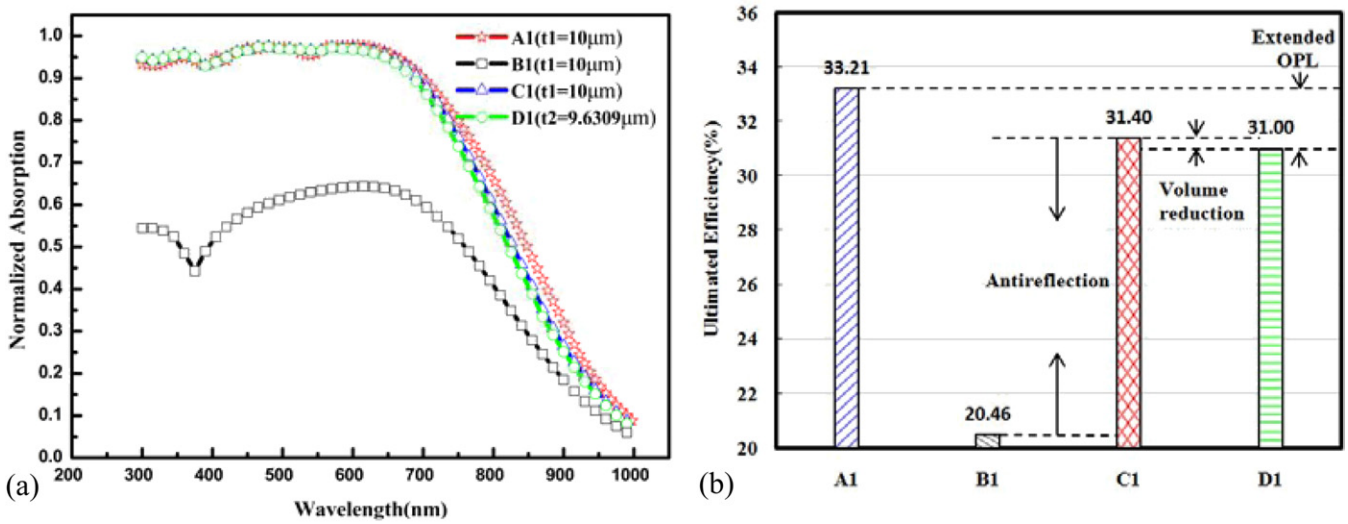

Figure 5. (*a*) Normalized absorption spectra. (*b*) Ultimate conversion efficiency and physics mechanisms for models A1, B1, C1 and D1 ($t1 = 10\,\mu$m, $t2 = 9.6309\,\mu$m).

intensity, which indicates that the extended OPL induced by high-order diffraction of the NCG structure plays an important role in such absorption enhancement.

The ultimate efficiency of the above-mentioned models at AM1.5 calculated according to equation (1) is shown in figure 5(*b*). Significantly, the ultimate efficiency of all models is higher than that of their counterparts in figure 3(*b*) due to their thicker active layer. Moreover, the ultimate efficiency of models A1, C1 and D1 is between 30% and 35%, much higher than that of the bare planar Si, which indicates that the front-interface reflection plays an important role in this efficiency enhancement. In order to accurately evaluate the efficiency enhancement, each physics mechanism induced by the NCG structure is listed in figure 5(*b*) where it makes a contribution to the efficiency. Compared with the value in figure 3(*b*) at $t1 = 1\,\mu$m and $t2 = 0.6309\,\mu$m, the efficiency degradation induced by volume reduction reduces from 3.16% to 0.40%, but the efficiency enhancement induced by antireflection increases from 5.36% to 10.95%, while the contribution of the extended OPL to the efficiency enhancement changes little. Overall, the front-interface reflection dominates the enhancement of absorption and efficiency for such thicker solar cells with a PML back-interface.

3.2.2. Air back-interface. The normalized absorption of models A2, B2, C2 and D2 is shown in figure 6(*a*). As air is their back-interface, models A2 and B2 are the real operation states for the 10 μm thick planar bare Si and NCG-textured Si solar cells, respectively. Significantly, figure 6(*a*) shows that the normalized absorption of models A2, C2 and D2 is nearly overlapped and much higher than that of model B2, when λ_{in} is less than 650 nm, which indicates that antireflection dominates their absorption, the volume reduction and guide-mode effect can be ignored over this span. Compared with figure 4(*a*), such a wavelength span dominated by antireflection is extended significantly because of their thicker active layer. Similarly, when $\lambda_{in} \geqslant 650$ nm, even though the cavity-resonance effect happens in all the above solar cells as ripples are observed, the absorption of model B2 is still lower than that of any other models, which indicates that antireflection is still the most effective method to improve their absorption and efficiency. Moreover, the nearly overlapped absorption spectrum of models C2 and D2 indicates that the influence of volume reduction on the absorption can be ignored when the active layer is as thick as 10 μm. Meanwhile, compared with other planar Si solar cells, considerably higher absorption is observed in the NCG-textured Si solar cell, as shown in figure 6(*a*), due to its guided-mode resonance effect induced by its specific high-order diffraction.

The ultimate efficiency of the above-mentioned models at AM1.5 calculated according to equation (1) is shown in figure 6(*b*). In order to accurately evaluate the efficiency enhancement, each physics mechanism resulting in the efficiency variation is marked in figure 6(*b*). The highest efficiency of 40.14%, 17.88% higher than that of model B2, is achieved in model A2. Therein, the contributions from antireflection, volume reduction and the guided-mode resonance effect are 11.31%, −0.21% and 6.36%, respectively, according to the difference in value of the corresponding models in figure 6(*b*). Significantly, antireflection induced by the NCG structure becomes the main source to improve the efficiency of Si solar cells, and the volume reduction effect can be ignored. In addition, a comparison of the models with different back-interfaces (PML and air) is shown in table 2. The contribution from the cavity-resonance effect to the efficiency enhancement is between 1.80% and 2.57% for all planar Si solar cells. It seems that the cavity-resonance effect is insensitive to the active layer thickness. For NCG-textured Si solar cells, the efficiency enhancement increases to 6.93%. There the contributions from the cavity-resonance effect and the guided-mode effect are 2.57% and 4.36%, respectively.

Compared with figure 4(*b*), the ultimate efficiency of all models in figure 6(*b*) is higher than that of their counterparts due to the thicker active layer. Moreover, it is worth noting that the efficiency of model A2 in figure 4(*b*) is 7.32% higher than

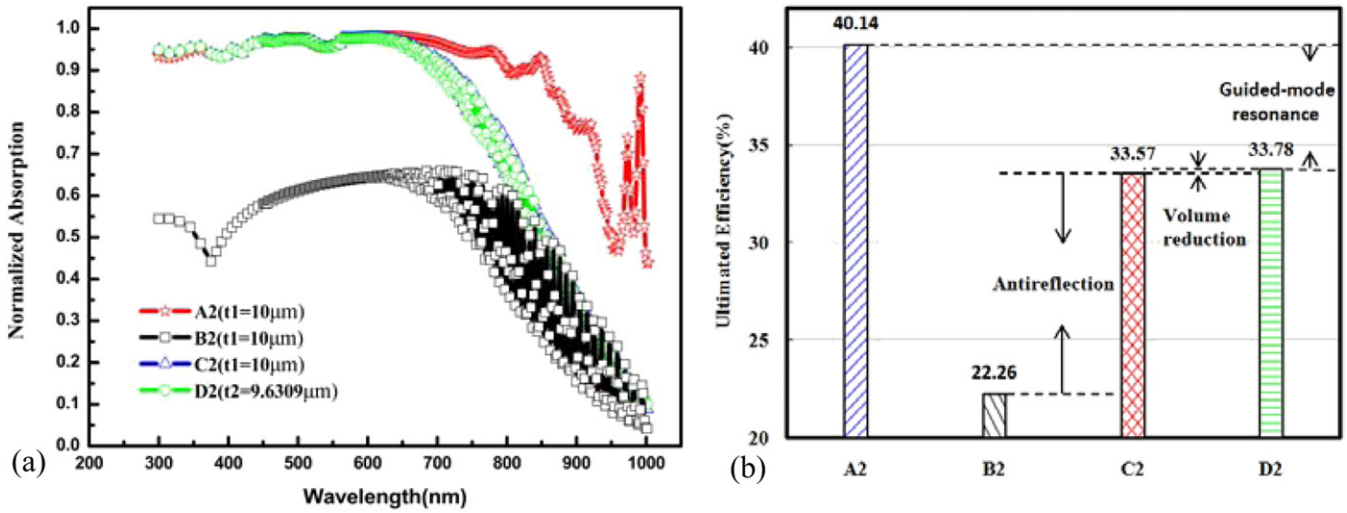

Figure 6. (*a*) Normalized absorption spectra. (*b*) Ultimate conversion efficiency for models A2, B2, C2 and D2 ($t1 = 10\,\mu$m, $t2 = 9.6309\,\mu$m).

Table 2. Comparison of efficiency of simulation models with different back-interfaces (PML and air) ($t = 10\,\mu$m).

η (%)	Model A	Model B	Model C	Model D
PML(1)	33.21	20.46	31.40	31.00
Air(2)	40.14	22.26	33.78	33.57
$\Delta\eta$ (%)	6.93	1.80	2.38	2.57

that of model B2 in figure 6(*b*). Such results further indicate that higher efficiency can be achieved in a much thinner active layer when the NCG structure is employed, which just meets the requirements of third generation photovoltaics. Moreover, the contribution from each physics mechanism to the efficiency is compared. When the active layer thickness changes from 1 to 10 μm, the efficiency degradation induced by volume reduction reduces from 3.16% to 0.21%, but the efficiency enhancement induced by the antireflection increases from 5.36% to 11.31%, while the contribution from the guided-mode resonance effect to the ultimate efficiency reduces from 16.01% to 6.36%. Therefore, the front-interface antireflection plays a more important role in the enhancement of absorption and efficiency of such thicker solar cells than that of thinner ones, while the guided-mode resonance effect is more beneficial to the thinner Si solar cells to improve their absorption and efficiency.

In order to further understand the influence of each physics mechanism on the efficiency enhancement of NCG-textured Si solar cells with different active layer thicknesses, the normalized efficiency contribution from every physics mechanism for the $t1 = 1\,\mu$m and $t1 = 10\,\mu$m samples is shown in figure 7. Significantly, the guided-mode resonance effect accounting for 54.17% of the total ultimate efficiency in such 1 μm thick NCG-textured Si solar cells surpasses the contribution from the planar Si itself, and dominates the efficiency of such solar cells. The efficiency from the antireflection and volume reduction accounts for 20.78% and -12.14% of the total ultimate efficiency, respectively. Any effect induced by such an NCG structure cannot be ignored

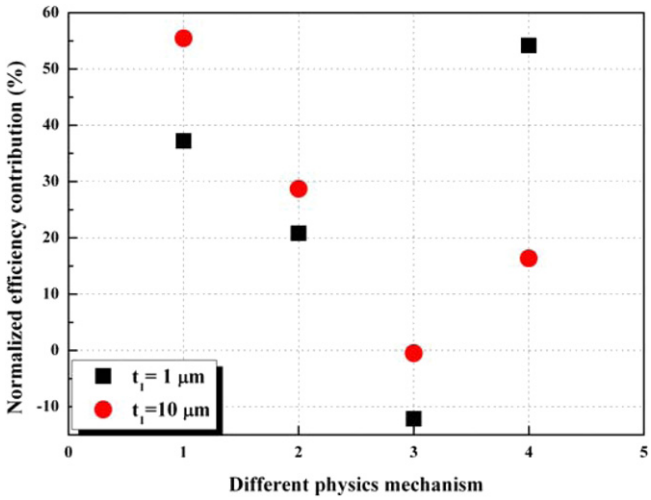

Figure 7. Normalized efficiency contribution from different physics mechanisms in NCG-textured Si solar cells with different active layer thicknesses (1: planar bare Si; 2: antireflection; 3: volume reduction; 4: guided-mode resonance effect).

in such 1 μm thick Si solar cells. The guided-mode resonance effect induced by high-order diffraction is not only the greatest factor of its efficiency enhancement, but also makes the largest contribution to the total efficiency. However, for a 10 μm thick NCG-textured Si solar cell, the planar Si structure makes the greatest contribution and accounts for 55.46% of the total ultimate efficiency due to its thicker active region. In the physics mechanisms induced by the NCG structure, the contribution from antireflection becomes greater, and accounts for 28.68% of the total efficiency, but the contribution from guided-mode resonance induced by high-order diffraction reduces down to 16.36%, and the volume reduction effect can be ignored, as shown in figure 7. Overall, in a thicker Si solar cell, antireflection, as the most important factor of absorption and efficiency enhancement, should be considered and carefully designed. However, in a thinner Si solar cell, the guided-mode resonance effect induced by

high-order diffraction dominates the ultimate efficiency. Such an accurate analysis benefits to further design and optimize nanotextured crystalline Si solar cells.

4. Conclusion

In summary, the absorption and efficiency contribution of the 1 μm and 10 μm thick NCG-textured Si solar cells are systematically simulated through four counterpart models with PML and air back-interfaces by RCWA and the TMM method, respectively. An optimized NCG structure with $P = 560$ nm and $H = 500$ nm is selected for the whole study. The contribution of each physics mechanism induced by the NCG structure to the absorption and efficiency is clearly investigated. The results indicate that the thinner the active layer, the larger the contribution from the guided-mode resonance effect to the ultimate efficiency. In particular, when the height of the nanostructures is equivalent to the active layer thickness, such a contribution can surpass that of the active layer itself. Meanwhile, the contribution from antireflection and volume reduction must also be considered. In contrast, the thicker the active layer, the larger the contribution from antireflection, and the lower the influence of volume reduction on the efficiency. In addition, the contribution from the cavity-resonance effect is quite weak and insensitive to the active layer thickness and back-interface reflection. This investigation provides a methodology for further delicately optimizing nanostructure-textured thin-film solar cells. Moreover, the further comparison shows that the efficiency of the 1 μm thick Si solar cell with the NCG structure is much higher than that of the 10 μm thick Si planar solar cell. This indicates that higher efficiency can be achieved in thinner Si solar cells by the use of an NCG structure, which just fulfils the requirements of third generation Si solar cells.

Acknowledgments

This work is funded by the National Natural Science Foundation (No 51202284), the Scientific Research Foundation for the Returned Overseas Chinese Scholars, State Education Ministry, the Jiangsu Province Project (No BE2009056) and the Suzhou City Project (No SG201020).

References

[1] Chutinan A, Kherani N P and Zukotynski S 2009 *Opt. Express* **11** 8871
[2] Dewan R and Knipp D 2009 *J. Appl. Phys.* **106** 074901
[3] Mutitu J G, Shi S, Chen C, Creazzo T, Barnett A, Honsberg C and Prather D W 2008 *Opt. Express* **16** 15238
[4] Garnett E and Yang P 2010 *Nano Lett.* **10** 1082
[5] Huang Y, Werf K H M, Houweling Z S and Schropp R E I 2011 *Appl. Phys. Lett.* **98** 113111
[6] Tsai M-A, Tseng P-C, Chen H-C, Kuo H-C and Yu P 2011 *Opt. Express* **19** A28
[7] Cao L, Fan P, Vasudev A P, White J S, Yu Z, Cai W, Schuller J A, Fan S and Brongersma M L 2010 *Nano Lett.* **10** 439
[8] Bao H and Ruan X 2010 *Opt. Lett.* **35** 3378
[9] Wang F, Yu H, Li J, Sun X, Wang X and Zheng H 2010 *Opt. Lett.* **35** 40
[10] Wang K X, Yu Z, Liu V, Cui Y and Fan S 2012 *Nano Lett.* **12** 1616
[11] Li J, Yu H, Wong S, Zhang G, Lo G-Q and Kwong D-L 2010 *J. Phys. D: Appl. Phys.* **43** 255101
[12] Wang B and Leu P W 2012 *Nanotechnology* **23** 194003
[13] Zhu J, Hsu C-M, Yu Z, Fan S and Cui Y 2010 *Nano Lett.* **10** 1979
[14] Hsu C-M, Battaglia C, Pahud C, Ruan Z, Haug F-J, Fan S, Ballif C and Cui Y 2012 *Adv. Energy Mater.* **2** 628
[15] Zhang R Y, Shao B, Dong J R, Zhang J C and Yang H 2011 *J. Appl. Phys.* **110** 113105
[16] Shockley W and Queisser H J 1961 *J. Appl. Phys.* **32** 510